Consistency of MODIS surface bidirectional reflectance distribution function and albedo retrievals:
1. Algorithm performance

Yufang Jin, Crystal B. Schaaf, Feng Gao,[1] Xiaowen Li,[1] and Alan H. Strahler
Department of Geography and Center for Remote Sensing, Boston University, Boston, Massachusetts, USA

Wolfgang Lucht
Potsdam-Institut für Klimafolgenforschung, Potsdam, Germany

Shunlin Liang
Department of Geography, University of Maryland, College Park, Maryland, USA

[1]   The first consistent year (November 2000 to November 2001) of global albedo product was produced at 1-km resolution every 16 days from the observations of the Moderate-Resolution Imaging Spectroradiometer (MODIS) instrument aboard NASA's Terra spacecraft. We evaluated the quality of the operational albedo retrievals in two ways: (1) by examining the algorithm performance using the product quality assurance (QA) fields (this paper) and (2) by comparing retrieved albedos with those observed at ground stations and by other satellite instruments (in a companion paper). The internal diagnostics of the retrieval algorithm adequately reflect the goodness of the model fit and the random noise amplification in the retrieved albedo. Global QA statistics show that the RossThick-LiSparse-Reciprocal model fits the atmospherically corrected surface reflectances very well, and the random noise amplification factors for white sky albedo and reflectance are generally less than 1.0. Cloud obscuration is the main reason for the activation of the backup magnitude retrieval algorithm. Over the 60°S to 60°N latitude band, 50% of the land pixels acquire more than six clear looks during 14–29 September 2001, and only 5% of these pixels are inverted with the backup algorithm. The latitude dependence and temporal distribution of the QA fields further demonstrate that the retrieval status mainly follows the pattern of angular sampling determined by cloud climatology and the instrument/orbit characteristics. A case study over the west coast of the United States shows that white sky shortwave albedos retrieved from magnitude inversions agree on average with those from full inversions to within 0.033 in reflectance units and have a slightly lower bias ranging from 0.014 to 0.023. We also explored the effect of residual cloud and aerosol contamination in the atmospherically corrected surface reflectance inputs in another case study over southern Africa. The quality assurance procedure of the operational MODIS bidirectional reflectance distribution function and albedo algorithm compensates for some of these residual effects and improves the albedo retrieval results by an order of 0.005 (10%) in the visible for more than 12% of pixels.   *INDEX TERMS:* 3322 Meteorology and Atmospheric Dynamics: Land/atmosphere interactions; 3359 Meteorology and Atmospheric Dynamics: Radiative processes; 3360 Meteorology and Atmospheric Dynamics: Remote sensing; *KEYWORDS:* MODIS, bidirectional reflectance distribution function, surface albedo, algorithm evaluation

1.   Introduction

[2]   Surface albedo is defined as the fraction of incident solar radiation reflected by Earth's surface. It characterizes the radiative property of the surface and is a primary controlling factor for the surface energy budget [*Dickinson*, 1983]. A recent report of the *Intergovernmental Panel on*

---

[1]Also at Research Center for Remote Sensing, Beijing Normal University, Beijing, China.

Climate Change (*IPCC*) [2001] identifies surface albedo effect due to land use change as an important radiative forcing agent. Such change in land use, mainly by deforestation, appears to have produced a negative radiative forcing of -0.2 ± 0.2 Wm^{-2} [*Hansen et al.*, 1998]. Several simulation studies have also shown regional and global climate changes due to perturbations of a few percent in land albedo in tropical regions [*Nobre et al.*, 1991; *Lean and Rowntree*, 1997], in semiarid regions [*Charney et al.*, 1977; *Sud and Fennessy*, 1982; *Knorr et al.*, 2001], and in global land surface [*Lofgren*, 1995]. A consistent and accurate global albedo data set is hence essential to the investigation of the sensitivity of climate to various types of forcing and to the identification of the effects of human activities [*King*, 1999]. The increasing fineness of spatial resolutions from 100 km to 50 km (and even 10 km) in modern climate models also calls for a high-resolution albedo inventory or a spatially explicit albedo specification [*Hahmann and Dickinson*, 2001]. It was suggested that an absolute accuracy of 0.02–0.05 is desirable for the albedo characterization at spatial and temporal scales compatible with climate studies [*Henderson-Sellers and Wilson*, 1983; *Sellers*, 1993].

[3] Traditionally, climate models rely on a global land cover map and a set of compiled field measurements to prescribe the surface albedo. However, significant albedo differences were shown to occur in various models due to complex observation conditions and inconsistent land cover classifications [*Henderson-Sellers and Wilson*, 1983]. Land surface models such as NCAR LSM [*Bonan*, 1996], BATS [*Dickinson et al.*, 1993], and SiB2 [*Sellers et al.*, 1996], adopt a two-stream approximation to calculate the surface albedo, which still depend on an accurate parameterization of the soil and vegetation system. Satellite remote sensing provides an efficient tool for a consistent global albedo characterization with high spatial and temporal resolutions. Atmospheric correction, directional-to-hemispherical conversion, and spectral interpolation, however, are the main sources of uncertainties in the retrieval of surface albedo from space.

[4] The Moderate-Resolution Imaging Spectroradiometer (MODIS), a key instrument aboard NASA's Terra (EOS AM-1) satellite, acquires global data in 36 spectral bands every one to two days. The rich spectral information improves our understanding of the Earth's atmosphere and reduces the uncertainty of atmospheric correction [*Justice et al.*, 1998]. The utilization of a surface bidirectional reflectance distribution function (BRDF) model [*Lucht et al.*, 2000] further improves the quality of surface albedo retrievals, compared to retrievals under a Lambertian assumption [*Hu et al.*, 1999]. Moreover, comprehensive quality assurance (QA) fields are embedded in the various levels of MODIS products and are taken into account in the higher-level processing streams [*Justice et al.*, 1998]. These advances make the MODIS BRDF and albedo products of particular value for global albedo characterization.

[5] Any satellite-derived products are not directly measured and hence an after-launch evaluation is critical for the assurance of product quality [*Justice and Townshend*, 1994]. The retrieval quality is essential to the user communities, without which the subsequent science would be open to question. In particular, the global performance of the albedo retrieval algorithm and the uncertainties of the albedo product must be addressed before the climate community is able to accept and correctly apply the global albedo data set in their modeling efforts. The evaluation also helps algorithm developers accordingly to refine the product in the future [*Schaaf et al.*, 2002].

[6] In this study we use the first consistent year (November 2000 to November 2001) of reprocessed MODIS BRDF and albedo products to investigate the performance of the MODIS BRDF and albedo retrieval algorithm. A detailed analysis of the quality assurance (QA) fields associated with the MODIS products serves as the internal diagnostics of the retrieval algorithm. We particularly address the effects of sparse angular sampling and atmospheric correction uncertainties on the MODIS surface BRDF and albedo products. Global statistics of the algorithm performance are also generated and analyzed. This study is the first part of our ongoing evaluation of operational MODIS BRDF and albedo products. In an accompanying paper [*Jin et al.*, 2003], we use the field measurements to assess the accuracy of the MODIS BRDF and albedo product and also examine its consistency with two commonly used global albedo products derived from other sensors.

2. MODIS BRDF and Albedo Retrieval Algorithm

2.1. Atmospherically Corrected Directional Reflectances

[7] A directional sampling of surface reflectances from MODIS can only be obtained by the accumulation of sequential observations over a specified time period. Cloud obscuration routinely reduces the number of clear looks. We chose a 16-day period as a trade-off between the sufficiency of angular samples and the stability of surface reflectivity [*Wanner et al.*, 1997; *Gao et al.*, 2001]. The well specified MODIS spectral bands improve the quality of cloud, aerosol, and water vapor retrievals. The high spatial resolution of the MODIS instrument also reduces the sub-pixel cloud contamination problem commonly found in the surface reflectances derived from coarse resolution sensors. By incorporating the atmospheric products in the atmospheric correction procedure, the uncertainty of MODIS surface reflectances is significantly reduced [*Vermote et al.*, 1997, 2002]. The theoretical typical relative error of surface reflectance ranges from 10% to 33% in the red and 3% to 6% in the near infrared, and is generally higher in cases of high aerosol loading and over sparsely vegetated areas [*Vermote et al.*, 1997]. The MODIS surface reflectance product contains extensive QA fields on cloud information, aerosol status, and spatial aggregation characteristics.

2.2. RossThick-LiSparse-Reciprocal BRDF Model

[8] The reflectance of naturally occurring land surface types is anisotropic and a BRDF model is employed to derive surface albedo from a limited number of angular samples [*Roujean et al.*, 1992; *Walthall et al.*, 1985; *Rahman et al.*, 1993; *Wanner et al.*, 1997]. The MODIS BRDF and albedo algorithm adopts the three-parameter, kernel-driven, RossThick-LiSparse-Reciprocal (RTLSR) BRDF model to characterize the directional distribution of surface reflectance. A volumetric kernel and a geometric kernel

represent two scattering patterns typified by homogeneous dense vegetation and by discrete shadow-casting objects, respectively. The readers are referred to *Wanner et al.* [1995] and *Lucht et al.* [2000] for detailed kernel derivations and expressions. The capacity of the RTLSR model to represent BRDF shapes was validated with field measurements over a variety of land cover types [*Hu et al.*, 1997]. *Privette et al.* [1997] and *Bicheron and Leroy* [2000] also demonstrated the high accuracy and efficiency of the RTLSR model inversion with sparse directional samplings from both field and satellite measurements. The small number of required parameters and the linear property of the RTLSR model is advantageous for operational BRDF and albedo retrievals from space on a global basis and at high spatial-temporal resolutions.

2.3. Inversion Strategy

2.3.1. Linear Regression

[9] The inversion strategy of the MODIS BRDF retrieval is to minimize the squared errors between model predicted and observed reflectances. The merit function of the inverse problem can be written as the following matrix:

$$Minimize\left\{(M_{n\times1} - K_{n\times3}X_{3\times1})^T C_E(M_{n\times1} - K_{n\times3}X_{3\times1})\right\}, \quad (1)$$

where M is the measurement vector in n different viewing and illuminating geometry, K is the kernel matrix, and X is a vector of kernel coefficients to be derived, and C_E is the measurement covariance matrix [*Lucht et al.*, 2000]. Note that the noise in atmospherically corrected surface reflectances is not quantitatively estimated. However, to take into account the uncertainty in input data, the MODIS BRDF and albedo processing stream first checks the QA fields of surface reflectance product, rejects any cloudy and high aerosol-loaded pixels, and assigns penalties to those observations with a lower quality [*Schaaf et al.*, 2002]. Furthermore, a possible outlier can be detected and discarded before the inversion begins.

[10] The BRDF is an intrinsic property of surface reflectance, depending only on canopy structure and elemental optical properties, whereas the actual surface albedo is affected by atmospheric illumination conditions. MODIS derives two intrinsic albedo products, black sky albedo (BSA) and white sky albedo (WSA), directly from the inverted RTLSR model. BSA (directional-hemispherical reflectance) refers to the special case of illumination from a collimated beam [*Martonchik et al.*, 2000]. It is derived through the angular integration of the BRDF over the full viewing hemisphere. WSA (bihemispherical reflectance) is similar in definition to BSA except that the illuminating radiation field is isotropic and covers the full illuminating hemisphere. The actual albedo occurring in nature can be approximated as a linear combination of BSA and WSA weighted by the fractions of direct and diffuse irradiance [*Lewis and Barnsley*, 1994]. Albedo is also wavelength-dependent. MODIS albedos are first derived for the 7 finite spectral bands (centered at 648, 858, 470, 555, 1240, 1640, and 2130 nm, respectively) and then spectral-to-broadband coefficients are used to derive three broadband albedos in the visible, near infrared, and total shortwave bands [*Liang et al.*, 1999].

2.3.2. Quality Assurance of MODIS BRDF and Albedo Product

[11] The covariance C_X of the parameters is given by $C_X = (K^T C_E^{-1} K)^{-1}$. In the ideal case of independent errors with equal variances σ^2, the covariance matrix is simplified as

$$C_X = (K^T K)^{-1}\sigma^2, \quad (2)$$

where $(K^T K)^{-1}$ describes the propagation of measurement noise to the BRDF parameters [*Gao et al.*, 2001]. Similarly, noise in measurements is propagated to any quantities derived from the BRDF parameters. Due to the linear property of the RTLSR BRDF model, the variance of reflectances and albedo can also be estimated analytically. *Lucht and Lewis* [2000] derived a so-called weight of determination (WoD) to represent the magnitude of noise amplification from measurements to reflectances and albedo. A WoD smaller than one means that the variance in retrieved quantities will be less than that in the original measured reflectances. The WoD is determined by the angular sampling and the kernel values at those angular geometries,

$$WoD = U^T (K^T K)^{-1} U, \quad (3)$$

where U is a vector composed of the weighting of the kernels, such as kernel values at given angles for the noise amplification in reflectances and angular integrals of kernels for the albedo noise amplification *Lucht and Lewis* [2000].

[12] The root mean square error (RMSE) is an indicator of the deviation of the RTLSR model fit from the atmospherically corrected surface reflectances. Two possible reasons for this residual error are noise inherent in the observations and the partial inability of the model to fit the observed reflectances. As part of the MODIS BRDF and albedo products, the RMSE and noise amplification factors for both nadir-view reflectance and white sky albedo are stored as several QA fields in each band. Table 1 summarizes the MODIS BRDF and albedo QA fields.

2.3.3. Backup Algorithm

[13] A backup algorithm (magnitude inversion) is implemented if there are insufficient angular samples or the internal quality check indicates a low confidence in the retrieval with the main algorithm. The basic concept behind the magnitude inversion is that the BRDF shapes for a certain land cover type are similar and thus can be prescribed. A global land cover classification, defined in terms of typical BRDFs, was derived from the Olson classification [*Olson*, 1994] and a seasonal model. The archetypal BRDFs for each land cover were compiled from various field measurements [*Strugnell and Lucht*, 2001; *Strugnell et al.*, 2001]. For each pixel, the corresponding archetypal BRDF is assumed as an a priori guess and a multiplicative factor is then derived from the available actual observations to adjust the a priori guess. Currently the archetypal BRDF database is being updated on a pixel-by-pixel basis and high quality BRDFs retrieved from MODIS full inversions are being used to replace the at-launch archetypes [*Schaaf et al.*, 2002].

3. Sampling Effects on MODIS BRDF and Albedo Retrievals

[14] Both the number and the variability of directional observations affect the quality of the BRDF retrievals

Table 1. Band-Specific Quality Assurance Fields in MODIS BRDF and Albedo Products (MOD43B)

Bit Fields	Value	RMSE	WoD (ref)	WoD (WSA)
0000	0	good	good	good
0001	1	good	good	moderate
0010	2	good	moderate	good
0011	3	good	moderate	moderate
0100	4	moderate	good	good
0101	5	moderate	good	moderate
0110	6	moderate	moderate	good
0111	7	moderate	moderate	moderate
1000	8	magnitude inversion	(num. obs. > = 7)	
1001	9	magnitude inversion	(num. obs. >3 and <7)	
1010	10	magnitude inversion	(num. obs.< = 3)	
1011	11	currently not used		
1111	15	fill value		

WoD(ref) and WoD(WSA) refer to noise amplification factor for nadir reflectance at $45°$ solar zenith angle and white sky albedo, respectively. Thresholds used for RMSE and WoD indicators are as follows: RMSE (good 0–0.10, moderate 0.10–0.20, poor > 0.40), WoD (good 0–0.75, moderate 0.75–1.25, poor > 2.00).

[*Privette et al.*, 1997]. In the MODIS BRDF and albedo QA fields, the number of clear looks is implicitly contained in the category of magnitude inversions or full inversions, and the distribution of angular sampling is partly represented by the weights of determination.

3.1. Spatial Distribution of the QA Fields

[15] Figure 1 shows the spatial distribution of the MODIS BRDF and albedo QA fields in the red band over the western United States (Tile h08v05: $30°N$ to $40°N$, $104°W$ to $130°W$) and over the Sahel region (Tile h18v07: $10°N$ to $20°N$, $0°E$ to $10°E$). The observation periods start in late May and middle September, respectively. In tile h08v05 (Figure 1a), the BRDF and albedo are retrieved with the highest quality (QA = 0) for the majority of pixels, and only small regions are retrieved with magnitude inversions using 4–6 clear observations (QA = 9). The pixels with a good RTLSR fit but moderate noise amplification (QA = 1) mainly occur adjacent to the regions with the magnitude inversion. Several small patches (QA = 8) occur in the east, where more than 6 clear looks are available but the magnitude inversion is performed.

[16] In tile h18v07 (Figure 1b), no retrievals, or retrievals with magnitude inversions using less than three clear looks, appear in the southern part. Moving towards the north, the number of clear looks increases and the retrieval status moves from the backup algorithm to the main algorithm. The rainy season in the Sahel region ($8°N$ to $18°N$, $17°W$ to $20°E$) occurs during the months of June through September when the Intertropical Convergence Zone (ITCZ) reaches its farthest northward extension ($15°N$). Also shown in tile h18v07 are apparent orbital boundaries indicating the effect of angular sampling geometry. Along the transitional area between the backup algorithm and the main algorithm, there are actually more than 7 clear looks but the main algorithm fails.

3.2. Case Studies of Sampling Effects

[17] To check the angular sampling patterns associated with the various QA designations, we selected individual pixels with various QAs and plotted their angular sampling as well as the individual surface directional reflectances in the red and near infrared. The observations of four such pixels in tile h08v05 (western United States) during May 25 to June 11, 2001 are shown in Figures 2 and 3. The QA flag

a). h08v05 (2001.145-160)

b). h18v07 (2001.257-272)
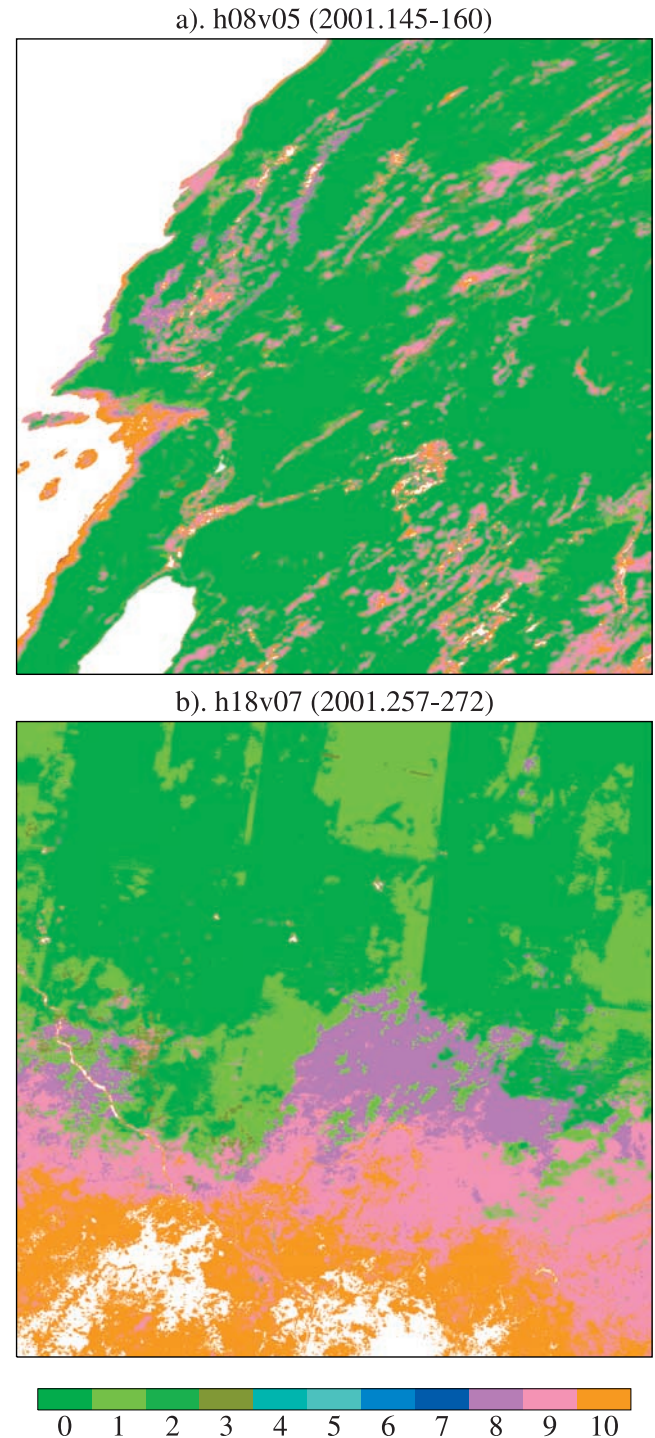
Figure 1. Images of MODIS BRDF and albedo QA in the red. MODIS tile h08v05 (Figure 1a) is in the west coast of the United States; the observations for BRDF and albedo retrieval are acquired within May 25 to June 11, 2001. MODIS tile h18v07 (Figure 1b) is in Sahara region and the observations are acquired within September 14 to September 29, 2001.

a). WoD=0.75 RMSE=0.005 QC=0

b). WoD=1.16 RMSE=0.005 QC=1
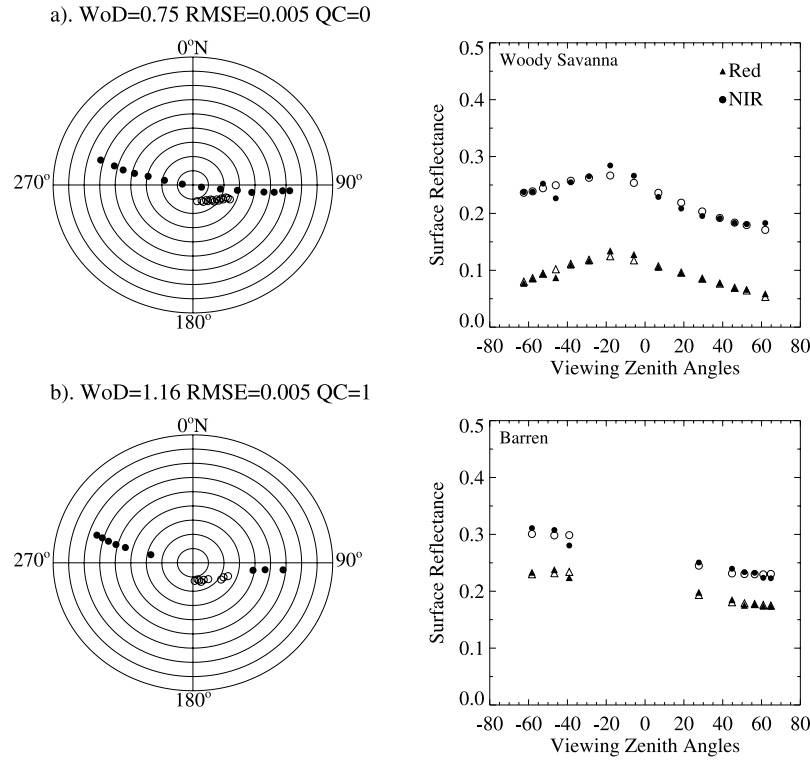
Figure 2. (a and b) MODIS angular samplings (left panels) and MODIS surface directional surface reflectance (right panels). The radius represents the zenith angle with an interval of 10° and the polar angle represents the azimuth. Solid circles refer to the viewing direction and open circles refer to the location of the sun. The weight of determination (WoD) for white sky albedo and root mean square error (RMSE) are also shown at the top of left panels as well as the QA field associated with the MODIS BRDF and albedo products. In the right panels, MODIS atmospherically-corrected surface reflectances are shown as solid symbols while those predicted by the MODIS BRDF model are shown as open symbols.

of Pixel 1 shows that it represents the best quality of inversion. The noise amplification factor is 0.75. Figure 2a shows how good its angular sampling is. Fifteen clear looks are available and its viewing zenith angles are evenly distributed from 0° to 60° in both forward and backward directions. The solar zenith angles range from 10° to 25° and the observations are mainly in the principal plane. The right panel of Figure 2a shows that the retrieved BRDF parameters predict well the surface reflectances observed by MODIS with the RMSE equal to 0.005. The hot spot phenomenon, a large peak in the backscattered radiation near the Sun's illumination direction arising from the absence of shadows in the direction of sensor [*Roujean*, 2000], is evident in the red and near infrared near 20 viewing zenith angle in the backward scattering direction.

[18] Compared to Pixel 1, Pixel 2 lacks the sampling between 0° to 40° in the backward direction and between 0° to 20° in the forward direction (Figure 2b). The QA flag indicates the noise amplification factor for white sky albedo is larger than that of Pixel 1. Pixel 3 has smaller ranges of viewing zenith angles and thus the noise amplification for both white sky albedo and nadir reflectance are relatively large (Figure 3a). For Pixel 4, viewing angles cover only the forward direction and the retrieval uncertainty is very sensitive to the noise of input data. The QA flag clearly indicates that the full inversion would be of such low quality that a magnitude inversion is made although there are more than seven clear looks available.

[19] We also examined a transitional area in tile h18v07 in Sahel, where there are a sufficient number of clear looks but the main algorithm still fails. For some pixels, the angular sampling is mainly distributed in the forward direction as in Pixel 4. The others cover a sufficient range of viewing angles as does Pixel 1, but MODIS acquires observations closer to the cross principal plane over North Africa in September. In this case, the WoD and hence the noise amplification are slightly higher than those of Pixel 1 and the algorithm turns to a magnitude inversion since a fixed threshold is set for the quality check.

[20] The above analysis shows that the QA fields of MODIS BRDF and albedo products characterize the angular sampling pattern and indicate the confidence and the processing stream of the inversion. To utilize the highest quality MODIS BRDF and albedo products, the users should check this QA information.

3.3. Full Inversion Versus Magnitude Inversion

[21] To examine the stability of the retrieval and the effect of the angular sampling on the albedo values, we plotted temporal sequences of albedo during 2001 in the red and near infrared narrowbands for six pixels in h08v05 (Figure 4). The time series of albedo are generally smooth for evergreen needleleaf forests in both the red and near infrared. The seasonal change of albedo is apparent for mixed forests, shrublands, savannas, grasslands, and croplands, especially in the near infrared band where leaf chlorophyll has very low
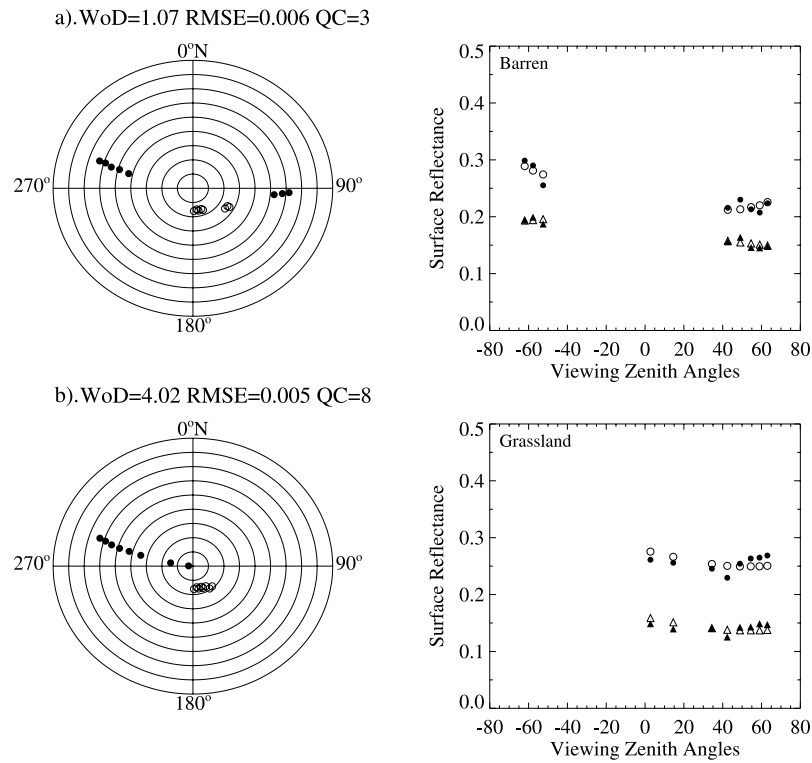
Figure 3. (a and b) Same as Figure 2, but for other pixels with different quality assurances.

absorption. Specifically, for these land cover types, albedo values in the near infrared start to increase in late April, become stable in summer, and then began to decrease in September. Obviously the time series of albedo capture the phenology of vegetation.

[22] A small number of apparently spurious retrievals are also shown on the temporal plots. We checked the corresponding QAs and identified the QAs with values greater than 3 in Figure 4. We found that lower quality magnitude inversions are the primary reason for these anomalous values. For the open shrubland pixel (Pixel 3, Figure 4b), for example, high quality full retrievals are obtained over Julian days 193–208 and 225–240, whereas the magnitude inversion is undertaken with only 4–6 clear looks available between these two periods. In this case, the albedo values are similar for the first and third time periods but are lower by up to 0.05 in the red and near infrared during the second time period. For pixel 3, we also noted a less abrupt decrease of the near infrared albedo by 0.025 over Julian days 129–145 compared to that over Julian days 113–128, although QAs indicate retrievals of good quality during growing season. It is probably due to the systematic atmospheric correction error in surface reflectances acquired over Julian days 129–145.

[23] To further investigate the difference between the retrievals from the main algorithm and the backup algorithm, we extracted all the pixels in tile h08v05 that have high quality full inversions for both the 193–208 and 225–240 time periods but are retrieved with magnitude inversions within Julian days 209–224 for each IGBP land cover type. The top panels of Figures 5–6 show the scatterplots of the albedo retrieval from the magnitude inversion versus that from the main algorithm for open shrublands and

barren, respectively. Generally the magnitude inversion agrees well with the full inversion. The correlation coefficient is above 0.94 and the RMSE is less than 0.033. The top panels show that the broadband white sky albedo from the magnitude inversion has a slightly lower bias of 0.014 in the visible and 0.023 in the near infrared for open shrublands. For barren areas, this lower bias is 0.017 and 0.019, respectively. To examine if this bias is caused by surface change from one period to the next, we plotted the full inversion albedos from the 193–208 period against those from the 225–240 time period in the bottom panels of Figures 5–6. The albedos from two time periods of full inversion are clearly in better agreement than the albedos from full and magnitude inversion. The above analysis indicates that the magnitude inversion results in a lower albedo bias over shrublands and barren. This bias may result from differences between the BRDF archetype and the actual BRDF. Currently the BRDF database is being updated with actual MODIS based parameters of the highest quality, which will reduce the uncertainty of BRDF archetypes [*Schaaf et al.*, 2002]. Also note that the magnitude inversion is more sensitive to noise in atmospherically corrected surface reflectances, especially when the number of observations is very small.

4. Effect of Atmospheric Correction Uncertainties on BRDF and Albedo Retrievals

4.1. Residual Atmospheric Effects in Surface Reflectances

[24] In addition to insufficient independent samples, possible noise in the atmospherically corrected surface reflectances may contribute to the uncertainty of the BRDF and
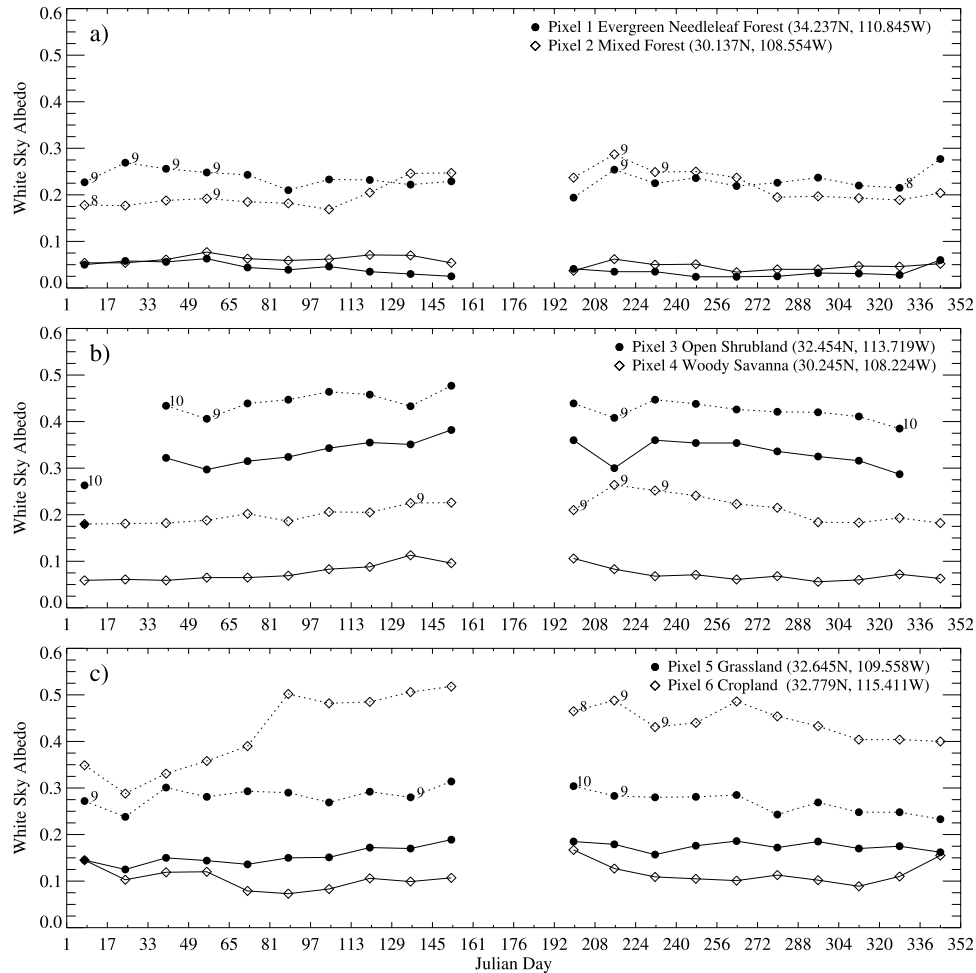
Figure 4. (a–c) Time series of surface white sky albedos during 2001 in the red (solid line) and near infrared (dashed line) narrowbands for selected pixels. The QA values greater than 3 (thus of lower quality) are marked along the near infrared white sky albedo. Note that the missing data in June is due to the Power Supply 2 shutdown anomaly of the MODIS instrument from 15 June 2001 to 2 July 2001.

albedo retrievals. It is clear that an exact assessment of the uncertainty of atmospheric correction and its effect on the BRDF and albedo retrievals can only be undertaken in conjunction with the validation of the atmospheric products. Moreover, the accuracy of both the atmospheric products and the atmospheric correction vary from region to region and time to time. Quality assessment thus becomes a challenging task. Various efforts are being undertaken to assess the accuracy of the atmospherically corrected surface reflectance product [*Vermote et al.*, 2002; *Liang et al.*, 2002]. *Liang et al.* [2002] used ground measured aerosol optical depth and water vapor content to perform atmospheric correction over the Beltsville Agricultural Research Center (BARC) agricultural test site, one of the EOS core validation site, and found that the MODIS surface reflectances agree well with their results. The typical relative error is within 5%.

[25] The relative accuracy of the atmospherically corrected surface reflectances is generally lower in cases of high aerosol loading and over sparsely vegetated areas [*Vermote et al.*, 1997]. As a case study, we examine if there is some residual effect from cloud or aerosol contamination in the surface reflectance product over semiarid regions. We chose an southern Africa tile (h20v10) as an example. Figure 7 shows the directional reflectances in the red and near infrared for a cropland pixel. There are 11 clear observations (no cloud, no cloud shadow, no high aerosol loading) as indicated by the QA fields associated with the MODIS surface reflectance product. The angular samplings are between the principal and cross principal plane. The NDVI values of the majority of the observations are in the range of 0.5–0.65, except for three observations marked as 1,2,3 in the figure. The surface reflectance of the marked observation 1 is extremely high in all visible bands and the NDVI is as low as 0.13. It is obviously contaminated by clouds. The NDVI values of observations 2 and 3 are 0.34, also much lower than those of the adjacent observations. Most probably, under-corrected aerosol increases their reflectance values and reduces their NDVI values.

4.2. Effects on BRDF and Albedo Retrievals

[26] To assure a best fit with those surface reflectances of higher quality, the current MODIS BRDF and albedo processing stream begins with a detailed check of each atmospherically corrected surface reflectance and assigns various penalty weights to the individual observations
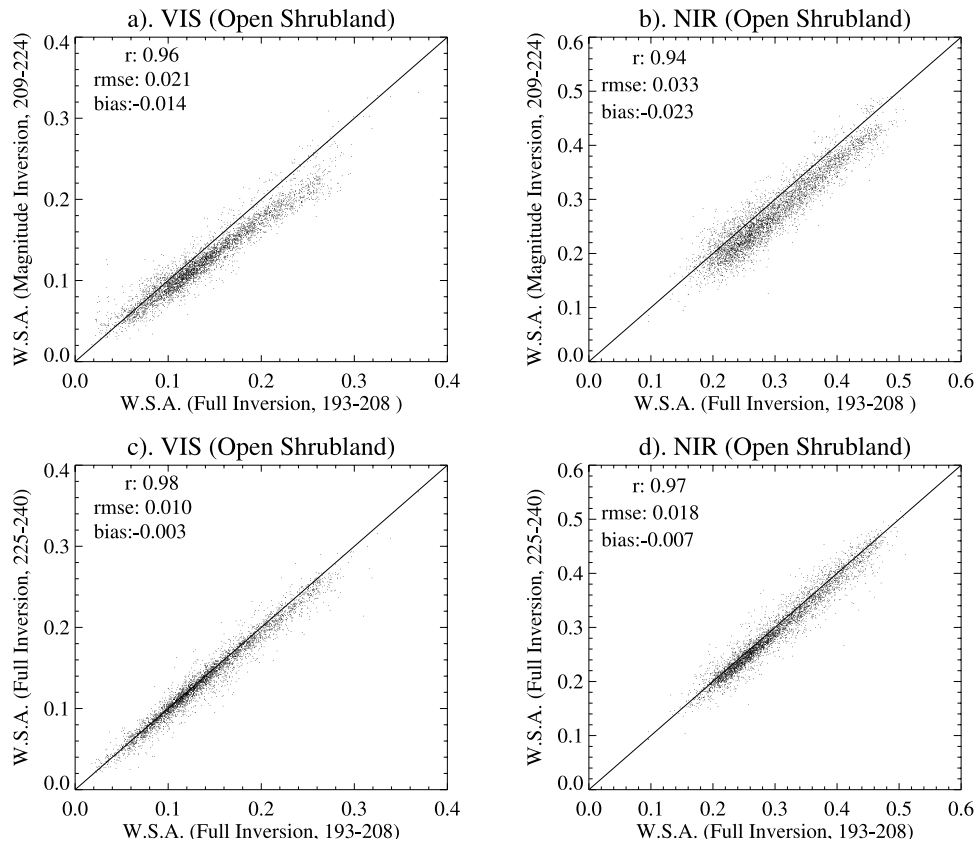
Figure 5. White sky albedos from magnitude inversion (backup algorithm) versus full inversion (main algorithm) in the visible (Figures 5a and 5c) and near infrared (Figures 5b and 5d) broadbands. Three consecutive 16-day periods are chosen to represent full inversion (193–208), magnitude inversion (209–224), and full inversion (225–240), respectively. Pixels shown are open shrublands.

according to the QA flag contained in surface reflectance product [*Schaaf et al.*, 2002]. For example, observations with high aerosol quantities are rejected and observations corrected with only aerosol climatology are assigned a penalty. Furthermore, one possible outlier is discarded and additional quality checks are then performed to assure that the BRDF parameters remain positive.

[27] For the pixel shown in Figure 7, the most apparent outlier, observation 2, is discarded. The BRDF parameters retrieved with the remaining observations are then all positive. Figure 7 shows how well the observed reflectances fit the reflectances predicted by the MODIS BRDF parameters and how the effects of the three contaminated observations are adjusted. The predicted bidirectional NDVI curve is also smoother than that derived from the original surface reflectances. However, if the most serious outlier is included in the retrieval, the inversion RMSE is very high and the shape of the BRDF appears incorrect. This indicates that the MODIS quality assurance process, the outlier detection in particular, improves the quality of MODIS BRDF retrievals.

[28] To further investigate to what degree the MODIS albedo product is improved by undertaking the quality assurance process, we calculated the relative and absolute differences between the operational MODIS white sky albedos and those retrieved without any checks or constraints for the entire tile h20v10. The histogram of relative difference (Figure 8) shows that the QA procedure has the

largest impact in the blue band. The MODIS white sky albedo agrees with the albedo retrieved without quality checks or constraints to within 10% for 88% of pixels in the green, 82% in the red, and 99% in the near infrared. We infer that the retrievals of around 20% of pixels are improved by taking into account the uncertainties in the surface reflectance product and by constraining the BRDF models in the visible bands.

4.3. Uncertainties of BRDF and Albedo Retrievals

[29] The MODIS BRDF and albedo processing mainly relies on the QA fields of the surface reflectance product and its internal quality checks to take the quality of the input data into account. A new retrieval method has recently been developed to assign weights to each observation based on the bidirectional NDVI values through an iterative procedure [*Gao et al.*, 2002]. It does not need ancillary information and higher weights are given to observations acquired under relatively clearer conditions. For the pixel shown in Figure 7, this method produces surface reflectances and albedos similar to those of the MODIS product. We consider that the retrievals by this algorithm provide a way to independently test the quality assurance. The difference between the retrievals using the biNDVI-based iterative algorithm and the operational MODIS albedo products can thus be taken as the uncertainties of the MODIS albedo products in a relative sense. The analysis of the retrievals for the tile h20v10 in late May shows that both agree within
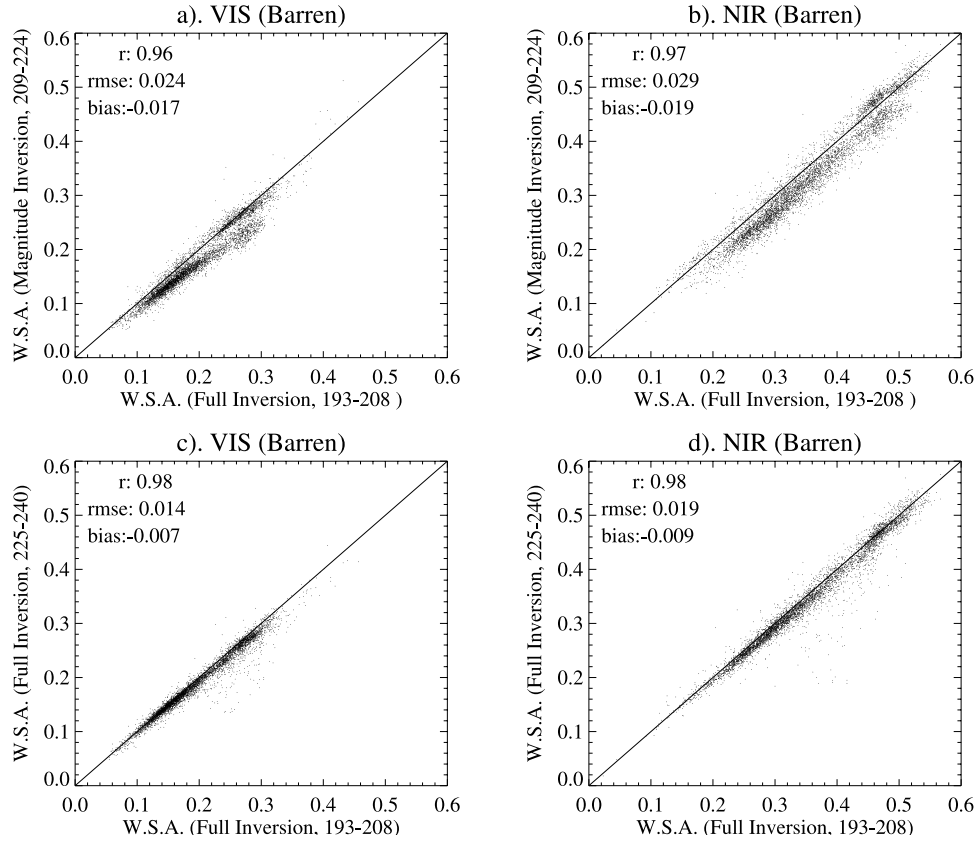
Figure 6. Same as Figure 5, but for barren pixels.

10% for 86% of pixels in the red, 93% of pixels in the green, and 61% of pixels in the blue. This implies that the uncertainties from atmospheric correction are generally within 10 percent in the green and red bands. The largest impact is found in the blue, whereas the smallest impact is in the near infrared with the relative difference less than 5%.

5. Global Performance of MODIS BRDF and Albedo Retrieval Algorithm

### 5.1. Global Statistics and Latitude Distribution

[30] To examine the performance of the MODIS BRDF and albedo retrieval algorithm over the globe, we analyzed the global reprocessed 1-km data acquired between September 14 to September 29, 2001. A land mask was applied to calculate the QA statistics for only the land pixels. Over the latitude bands between 60°N and 60°S, 50% of the land pixels receive more than 6 clear looks during this 16 day period and among these there are only 5% of pixels where the backup algorithm is performed instead of the main algorithm. Poor sampling and the contamination of atmosphere are the main reasons for the failure of the main algorithm in such cases. In total, 47% of the land pixels are retrieved with the full inversion, 45% with the magnitude inversion, and 8% cannot be retrieved. It is obvious that the loss of observations due to cloud cover is the main reason for the use of the backup magnitude inversion. Among those pixels with full inversion retrievals, the RTLSR model fits the atmospherically corrected surface reflectance very well for 99.9% of pixels, the noise ampli-

fication factor of white sky albedo is very small (less than 0.10) for 87% of pixels, and the noise amplification factor of nadir-view reflectances is very small (less than 0.75) for 74% of pixels. This indicates that the majority of pixels have very reliable albedo retrievals.

[31] Figure 9 shows that the latitude distribution of the magnitude retrievals and non-retrievals follows the pattern of cloud climatology in September 2001. Around 70% of pixels obtain less than 4 clear looks in the ITCZ zone between 10°S to 10°N, and around 35% of pixels between 10°S to 20°S and between 10°N to 20°N. Over the region 40°N to 30°S, the majority of the full-inversion pixels are retrieved with very high confidences (QA = 0) for both white sky albedo and nadir-view reflectance. We found that the MODIS angular sampling is closer to the principal plane over these latitude bands than it is in the more northern or southern tiles.

5.2. Temporal Distribution

[32] In addition to the latitude dependence, the angular sampling varies with season due to orbital change and cloud dynamics. Due to the large data volume of the global data at 1-km resolution, we chose several tiles to investigate the dynamics of the performance of the MODIS BRDF and albedo retrieval algorithm. Figure 10 shows the temporal distribution of the retrieval status in 2001 for a tile over the west coast of the United States (h08v05), which is usually less cloudy than other regions. It is obvious that the number of the pixels retrieved with the magnitude inversion is larger in winter because of higher frequency of cloud cover in this
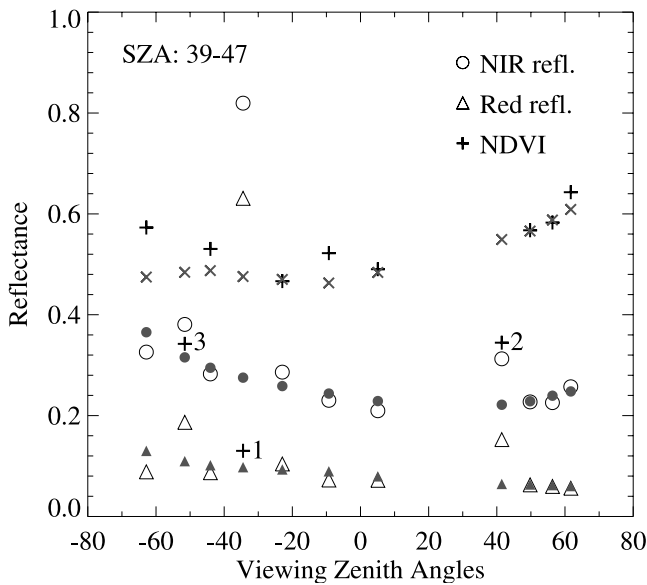
Figure 7. MODIS atmospherically corrected surface reflectances in the red (open triangles) and near infrared (open circles) and NDVIs (pluses). Values are for a cropland pixel located in MODIS tile h20v10 (16.0041°S, 26.7056°E), sampled during May 25 to June 11, 2001. Three cloud/aerosol contaminated observations are marked besides their extremely low NDVI values. The reflectances and NDVIs predicted by the MODIS retrieved BRDF parameters are represented by solid symbols and crosses. Shown here is the good prediction ability of the operational MODIS BRDF product with the quality-assurance procedure.

region during this time than in other seasons. In addition, the most significant change in angular geometries happens in the azimuthal dimension during various seasons. In tile h08v05, for example, the angular sampling is closer to the principal plane in spring and summer and then moves towards the cross principal plane in fall. Figure 10 shows that the majority of the pixels with more than 6 clear looks have the highest confidence of retrieval in spring and summer, whereas the pixels with moderate noise amplification factors increase in fall and winter, and the percentage of main algorithm failure to fit the observations also increases. It is well known that the anisotropy of canopy reflectance is more apparent in the principal plane and thus the RTLSR model is more sensitive to the observations in the principal plane and the accuracy of the BRDF inversion tends to be higher.

6. Discussions and Summary

[33] The operational MODIS BRDF and albedo products became provisional with the data from 31 October 2001 [*Schaaf et al.*, 2002]. A detailed evaluation is critical for the correct interpretation and usage of the product by the science community. This study used the first consistent year of MODIS reprocessed products to provide the evaluation of the performance of the MODIS BRDF and albedo retrieval algorithm. We found that the Quality Assurance (QA) fields embedded in the product adequately reflect the

processing stream, goodness of model fitting, angular sampling patterns, and random noise amplification of the retrieved BRDF and albedo products as well. Users of the product are therefore strongly advised to check these QA fields and to consider the specific quality requirement of an individual application. A case study, for example, showed that white sky albedos from the backup magnitude inversion algorithm agree with those from the main full inversion algorithm to within 0.033 in reflectance units, but have a slight bias toward lower values ranging from 0.014 in the visible to 0.023 in the near infrared broadband.

[34] We also examined the effect of the uncertainty of the MODIS atmospheric correction on the MODIS BRDF and albedo retrievals. Some residual cloud and aerosol effects were identified in atmospherically corrected surface reflectances from a case study in Southern Africa. However, in addition to using the QA information associated with the input surface reflectance product, the MODIS BRDF and albedo algorithm also performs a series of internal checks to avoid residual input problems and ensure high quality retrievals. Compared to the albedo retrieved without accounting for the quality of the input data and without constraints to avoid negative non-physical BRDF parameters, the operational MODIS white sky albedo is improved for around 15–20% of the pixels in the visible bands and for 10% of the pixels in the near infrared.

[35] The global statistics of the QA fields show that the MODIS BRDF and albedo retrieval algorithm generally performs quite well. During the period 14–29 September 2001 and over 60°S to 60°N, 50% of the land pixels acquire more than 6 clear looks and only 5% of these are ultimately inverted with the backup algorithm due to atmospheric contamination or an inability of the model to fit the observations. The RMSEs of the RTLSR model in fitting the atmospherically corrected surface reflectances are gen-
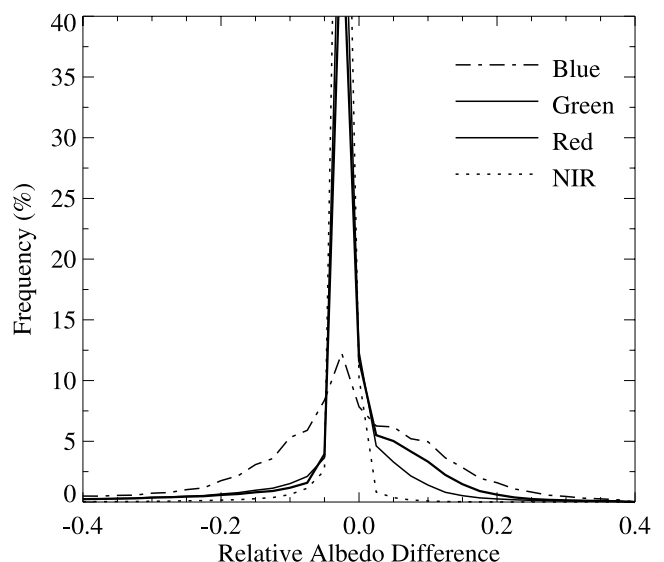
Figure 8. Histogram of relative differences between the operational MODIS white sky albedo and that derived without any quality check or BRDF parameter constraints in the blue, green, red and near infrared. Results are derived from MODIS observations in tile h20v10 during May 25 to June 11, 2001.
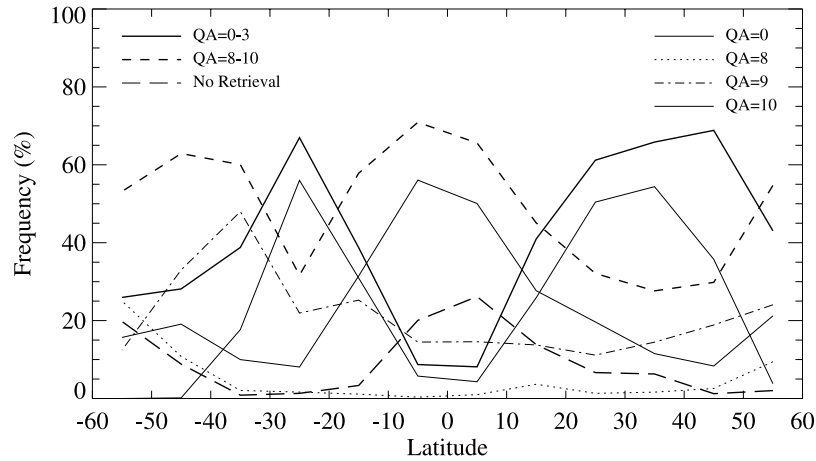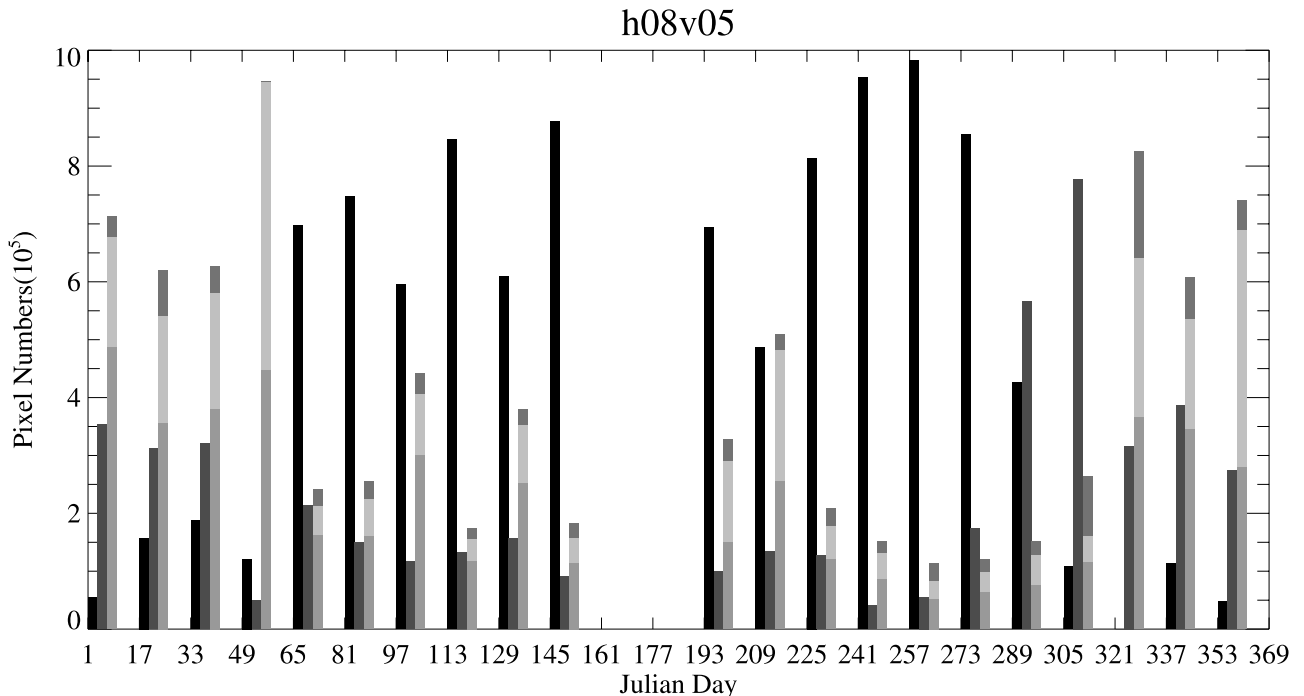
Figure 9. Latitude distributions of the frequency of BRDF and albedo retrieval status for September 2001. The solid line refers to the best quality of retrieval, the dashed line refers to all the magnitude inversions, and the long dashed line refers to no retrievals. Also shown are magnitude inversion with more than 6 looks (dotted), 3–7 looks (dashed-dotted) and less than three looks (dashed-dotted-dotted).

erally small. Among those pixels retrieved with full inversions, the random noise amplification factor of white sky albedo is very small (less than 0.75) for 87% of pixels and that of nadir-view reflectance is also very small for 74% of pixels. Our analysis shows that cloud cover poses the most serious problem to surface retrieval. In September, 8% of the pixels can not be retrieved due to an absence of clear observations and 45% rely on the backup magnitude retrieval. The percentage of pixels inverted with full inversions is expected to be lower in other seasons when the large land area in Northern Hemisphere is typically more cloudy.

[36] The latitude dependence and temporal distribution of the QA fields also show that the retrievals tend to be more reliable when the observations are closer to the principal plane. In view of this often insufficient angular sampling, a synergistic usage of multi-sensor observations is important to improve both the coverage and the quality of global albedo retrieval. The Multi-angle Imaging Spectroradiometer (MISR) [*Diner et al.*, 1998], aboard the same

Figure 10. Temporal distributions of the frequency of BRDF and albedo retrieval status for tile h08v05 in 2001. Three series of QA information are plotted: QA = 0; QA = 1–3; QA = 9 (bottom), 10 (middle), 8(top). The retrievals with moderate RMSEs (QA = 4–7) generally occupy less than 1% of the total land pixels and therefore are not included here.

EOS-Terra platform as MODIS, acquires observations almost perpendicular to those of MODIS in the azimuth plane and is thus of particular value for future improvement of MODIS BRDF and albedo product [*Jin et al.*, 2002]. A second MODIS instrument was launched on the EOS-Aqua platform and cloud free observations from this afternoon sensor will bring additional solar zenith angle variations to this synergism, which implies that the quality of the MODIS BRDF and albedo product will improve in the near future.

[37] The evaluation of algorithm performance here relied on the product QAs, analysis of the input data, and intercomparisons with results from different retrieval algorithms. In the second part of our evaluation study [*Jin et al.*, 2003], the MODIS albedo is validated with coincident field measurements from NOAA's Surface Radiation Network (SURFRAD) stations and from the Southern Great Plains (SGP) sites of the DOE's Atmospheric Radiation Measurement (ARM) Program. The global MODIS albedo is also compared to commonly used global albedo data sets derived from other sensors.

References

Bicheron, P., and M. Leroy, Bidirectional reflectance distribution function signatures of major biomes observed from space, *J. Geophys. Res.*, *105*, 26,669–26,681, 2000.

Bonan, G. B., A land surface model (LSM version 1.0) for ecological, hydrological, and atmospheric studies: Technical description and user's guide, *NCAR Tech. Note NCAR/TN-147+STR*, Natl. Cent. for Atmos. Res., Boulder, Colo., 1996.

Charney, J., W. J. Quirk, S. Chow, and J. Kornfield, A comparative study of the effects of albedo change on drought in semi-arid regions, *J. Atmos. Sci.*, *34*, 1366–1385, 1977.

Dickinson, R. E., Land surface processes and climate: Surface albedos and energy balance, *Adv. Geophys.*, *25*, 305–353, 1983.

Dickinson, R. E., A. Henderson-Sellers, and P. J. Kennedy, Biosphere-Atmosphere Transfer Scheme (BATS) Version 1e as coupled to the NCAR community model, *NCAR Tech. Note NCAR/TN-387+STR*, Natl. Cent. for Atmos. Res., Boulder, Colo., 1993.

Diner, D. J., et al., Multi-angle Imaging Spectroradiometer (MISR) instrument description and experiment overview, *IEEE Trans. Geosci. Remote Sens.*, *36*, 1072–1085, 1998.

Gao, F., C. B. Schaaf, A. H. Strahler, and W. Lucht, Using a multi-kernel least-variance approach to retrieve and evaluate albedo from limited bidirectional measurements, *Remote Sens. Environ.*, *76*, 57–66, 2001.

Gao, F., Y. Jin, X. Li, C. Schaaf, and A. Strahler, Bidirectional NDVI and atmospherically resistant BRDF inversion for vegetation canopy, *IEEE Trans. Geosci. Remote Sens.*, *40*, 1269–1278, 2002.

Hahmann, A. N., and R. E. Dickinson, A fine-mesh land approach for general circulation models and its impact on regional climate, *J. Clim.*, *14*, 1634–1646, 2001.

Hansen, J., M. Sato, A. Lacis, R. Ruedy, I. Tegen, and E. Matthews, Climate forcings in the industrial era, *Proc. Natl. Acad. Sci. U.S.A.*, *95*, 12,753–12,758, 1998.

Henderson-Sellers, A., and M. F. Wilson, Surface albedo data for climatic modeling, *Rev. Geophys.*, *21*, 1743–1778, 1983.

Hu, B., W. Lucht, X. Li, and A. H. Strahler, Validation of kernel-driven models for global modeling of bidirectional reflectance, *Remote Sens. Environ.*, *62*, 201–214, 1997.

Hu, B., W. Lucht, and A. H. Strahler, The interrelationship of atmospheric correction of reflectances and surface BRDF retrieval: A sensitivity study, *IEEE Trans. Geosci. Remote Sens.*, *37*, 724–738, 1999.

Intergovernmental Panel on Climate Change (IPCC), *Climate Change 2001: The Scientific Basis*, Cambridge Univ. Press, New York, 2001.

Jin, Y., F. Gao, C. B. Schaaf, X. Li, A. H. Strahler, C. J. Bruegge, and J. V. Martonchik, Improving MODIS surface BRDF/Albedo retrieval with MISR observations, *IEEE Trans. Geosci. Remote Sens.*, *40*, 1593–1604, 2002.

Jin, Y., C. B. Schaaf, C. E. Woodcock, F. Gao, X. Li, A. H. Strahler, W. Lucht, and S. Liang, Consistency of MODIS surface bidirectional reflectance distribution function and albedo retrievals: 2. Validation, *J. Geophys. Res.*, *108*, doi:10.1029/2002JD002804, in press, 2003.

Justice, C. O., and J. R. G. Townshend, Data sets for global remote sensing: Lessons learnt, *Int. J. Remote Sens.*, *15*, 3621–3639, 1994.

Justice, C. O., et al., The Moderate Resolution Imaging Spectroradiometer (MODIS): Land remote sensing for global change research, *IEEE Trans. Geosci. Remote Sens.*, *36*, 1228–1249, 1998.

King, M. D., *EOS Science Plan: The State of Science in the EOS Program*, Natl. Aeronaut. and Space Admin., Washington, D.C., 1999.

Knorr, W., K.-G. Schnitzler, and Y. Govaerts, The role of bright desert regions in shaping North African climate, *Geophys. Res. Lett.*, *28*, 3489–3492, 2001.

Lean, J., and P. R. Rowntree, Understanding the sensitivity of a GCM simulation of Amazonian deforestation to the specification of vegetation and soil characteristics, *J. Clim.*, *10*, 1217–1235, 1997.

Lewis, P., and M. J. Barnsley, Influence of the sky radiance distribution on various formulations of the Earth surface albedo, paper presented at International Symposium on Physical Measurements and Signatures in Remote Sensing, Int. Sco. for Photogramm. and Remote Sens., Val d'Isere, France, 1994.

Liang, S., A. H. Strahler, and C. W. Walthall, Retrieval of land surface albedo from satellite observations: A simulation study, *J. Appl. Meteorol.*, *38*, 712–725, 1999.

Liang, S., H. Fang, M. Chen, C. J. Shuey, C. Walthall, C. Daughtry, J. Morisette, C. Schaaf, and A. Strahler, Validating MODIS land surface reflectance and albedo products: Methods and preliminary results, *Remote Sens. Environ.*, *83*, 149–162, 2002.

Lofgren, B. M., Sensitivity of land-ocean circulations, precipitation, and soil moisture to perturbed land surface albedo, *J. Clim.*, *8*, 2521–2542, 1995.

Lucht, W., and P. Lewis, Theoretical noise sensitivity of BRDF and albedo retrieval from the EOS-MODIS and MISR sensors with respect to angular sampling, *Int. J. Remote Sens.*, *21*, 81–98, 2000.

Lucht, W., C. B. Schaaf, and A. H. Strahler, An algorithm for the retrieval of albedo from space using semiempirical BRDF models, *IEEE Trans. Geosci. Remote Sens.*, *38*, 977–998, 2000.

Martonchik, J. V., C. J. Bruegge, and A. H. Strahler, A review of reflectance nomenclature used in remote sensing, *Remote Sens. Rev.*, *19*, 9–20, 2000.

Nobre, C. A., P. J. Sellers, and J. Shukla, Amazonian deforestation and regional climate change, *J. Clim.*, *4*, 957–988, 1991.

Olson, J. S., Global ecosystem framework: Definitions, internal report, 37 pp., USGS EROS Data Cent., Sioux Falls, S.D., 1994.

Privette, J. L., T. F. Eck, and D. W. Deering, Estimating spectral albedo and nadir reflectance through inversion of simple BRDF models with AVHRR/MODIS-like data, *J. Geophys. Res.*, *102*, 29,529–29,542, 1997.

Rahman, H., B. Pinty, and M. M. Verstraete, Coupled surface-atmosphere reflectance (CSAR) model, 1, Model description and inversion on synthetic data, *J. Geophy. Res.*, *98*, 20,779–20,789, 1993.

Roujean, J.-L., A parametric hot spot model for optical remote sensing applications, *Remote Sens. Environ.*, *71*, 197–206, 2000.

Roujean, J. L., M. Leroy, and P. Y. Deschamps, A bidirectional reflectance model of the Earth's surface for the correction of remote sensing data, *J. Geophys. Res.*, *97*, 20,455–20,468, 1992.

Schaaf, C. B., et al., First operational BRDF, albedo and nadir reflectance products from MODIS, *Remote Sens. Environ.*, *83*, 135–148, 2002.

Sellers, P. J., Remote sensing of the land surface for studies of global change, NASA/GSFC International Satellite Land Surface Climatology Project report, NASA Goddard Space Flight Cent., Greenbelt, Md., 1993.

Sellers, P. J., D. A. Randall, G. J. Collatz, J. A. Berry, C. B. Field, D. A. Dazlich, C. Zhang, G. D. Collelo, and L. Bounoua, A revised land surface parameterization (SiB2) for atmospheric GCMs, part I, Model formulation, *J. Clim.*, *9*, 676–705, 1996.

Strugnell, N. C., and W. Lucht, An algorithm to infer continental-scale albedo from AVHRR data, land cover class, and field observations of typical BRDFs, *J. Clim.*, *14*, 1360–1376, 2001.

Strugnell, N. C., W. Lucht, and C. Schaaf, A global albedo data set derived from AVHRR data for use in climate simulations, *Geophys. Res. Lett.*, *28*, 191–194, 2001.

Sud, Y. C., and M. Fennessy, A study of the influence of surface albedo on july circulation in semi-arid regions using the glas gcm, *J. Clim.*, *2*, 105–125, 1982.

Vermote, E. F., N. Z. Saleous, C. O. Justice, Y. J. Kaufman, J. Privette, L. Remer, J. C. Roger, and D. Tarne, Atmospheric correction of visible to middle infrared EOS-MODIS data over land surface, background, op-

erational algorithm and validation, *J. Geophys. Res.*, *102*, 17,131–17,141, 1997.

Vermote, E. F., N. Z. E. Saleous, and C. O. Justice, Atmospheric correction of MODIS data in the visible to middle infrared: First results, *Remote Sens. Environ.*, *83*, 97–111, 2002.

Walthall, C. L., J. M. Norman, J. M. Welles, G. Campbell, and L. B. Blad, Simple equation to approximate the bidirectional reflectance from vegetative canopies and bare soil surfaces, *Appl. Opt.*, *24*, 383–387, 1985.

Wanner, W., X. Li, and A. H. Strahler, On the derivation of kernels for kernel-driven models of bidirectional reflectance, *J. Geophys. Res.*, *100*, 21,077–21,089, 1995.

Wanner, W., A. H. Strahler, B. Hu, P. Lewis, J.-P. Muller, X. Li, C. B. Schaaf, and M. J. Barnsley, Global retrieval of bidirectional reflectance and albedo over land from EOS MODIS and MISR data: Theory and algorithm, *J. Geophys. Res.*, *102*, 17,143–17,162, 1997.

————————————

F. Gao, Y. Jin, X. Li, C. B. Schaaf, and A. H. Strahler, Department of Geography and Center for Remote Sensing, Boston University, Boston, MA 02215, USA. (yfj@bu.edu; fgao@crsa.bu.edu; lix@crsa.bu.edu;schaaf@crsa.bu.edu; alan@bu.edu)

S. Liang, Department of Geography, 2181 LeFrak Hall, College Park, MD 20742, USA. (sliang@geog.umd.edu)

W. Lucht, Potsdam-Institut für Klimafolgenforschung (PIK), Telegrafenberg C4, Postfach 60 12 03, D14412 Potsdam, Germany. (wolfgang.lucht@pik-potsdam.de)